Indian J Phys (September 2017) 91(9):999–1011
DOI 10.1007/s12648-017-0996-0

ORIGINAL PAPER

Structural, electronic, mechanical, thermal and optical properties of $B(P,As)_{1-x}N_x$; (x = 0, 0.25, 0.5, 0.75, 1) alloys and hardness of B(P,As) under compression using DFT calculations

E Viswanathan, M Sundareswari*, D S Jayalakshmi, M Manjula and S Krishnaveni

Department of Physics (DST-FIST Sponsored), Sathyabama University, Chennai, Tamilnadu 600 119, India

Received: 26 September 2016 / Accepted: 17 January 2017 / Published online: 5 April 2017

Abstract: First principles calculations are carried out in order to analyze the structural, electronic, mechanical, thermal and optical properties of BP and BAs compounds by ternary alloying with nitrogen namely $B(P,As)_{1-x}N_x$ (x = 0.25, 0.5, 0.75) alloys at ambient condition. Thereby we report the mechanical and thermal properties of $B(P,As)_{1-x}N_x$ (x = 0.25, 0.5, 0.75) alloys namely bulk modulus, shear modulus, Young's modulus, hardness, ductile–brittle nature, elastic wave velocity, Debye temperature, melting point, etc.; optical properties of $B(P)_{1-x}N_x$ (x = 0.25, 0.5, 0.75) and $B(As)_{1-x}N_x$ (x = 0.25, 0.75) alloys namely the dielectric function of real and imaginary part, refractive index, extinction coefficient and reflectivity and the hardness profile of the parent compounds BP and BAs under compression. The charge density plot, density of states histograms and band structures are plotted and discussed for all the ternary alloys of the present study. The calculated results agree very well with the available literature. Analysis of the present study reveals that the ternary alloy combinations namely $BP_{.25}N_{.75}$ and $BAs_{.25}N_{.75}$ could be superhard materials; hardness of BP and BAs increases with compression.

Keywords: Covalent bonding; Superhard material; Semiconductor; Band gap; Optical properties and brittleness

PACS Nos.: 71.20.Nr; 78.20 Ci; 62.20 mj

1. Introduction

'Hardness' is one of the fundamental mechanical properties of materials and is defined as the property that enables the material to resist being scratched by another. Designing a supplementary hard/superhard material that is harder than diamond and c-BN is still under research. The combined effect of large coordination number, higher covalency between atoms and shorter bond length are the peculiar properties of conventional superhard materials. These materials find excellent technological applications in polishing tools, abrasives, cutting tools and wear-resistant/protective coating [1–3]. Historically III-V semiconductors especially, boron based compounds viz., BN, BP and BAs [4–16] are familiar for their excellent mechanical properties due to their smaller atomic radii and stronger polar directional bonding. Investigation of BP, BAs, BSb, BBi, c-BN, h-BN, B_2CN, BCN, B_2O, B_4C, BC_3 and BC_5 compounds shows that they have promising mechanical thermal, electrical properties, excellent thermal conductivity and a high thermoelectric power [4–16]. Further, comparative electronic and structural properties of BN, BP, BAs and BSb are reported by Zaoui et al. [17] in the year 2001; Bagci et al. [18] have reported the electronic and phonon properties of BP, BAs and BSb compounds. In parallel, many researchers have worked on boron based ternary materials by doping. Guemou et al. [19] have reported the structural and optical properties of ternary BN_xAs_{1-x} alloys. Origin of gap bowing in BN_xP_{1-x}, BN_xAs_{1-x} and BP_xAs_{1-x} alloy combinations are reported by El Haj Hassan et al. [20] in the year 2005. Bouhemadou et al. [21] have reported the elastic properties in zinc-blende III-P compounds under pressure effects in the year 2009. Further, Abdiche et al. [22] have discussed the structural and electronic properties of cubic quaternary $B_xGa_{1-x}As_{1-y}N_y$ alloys using the first principles calculation.

*Corresponding author, E-mail: sundare65@gmail.com

For the ternary alloys under present study namely $B(P,As)_{1-x}N_x$ (x = 0.25, 0.5, 0.75), only some of the optical properties are reported whereas their mechanical and thermal properties are not yet been discussed earlier in the literature. Hence, in the present study, we report on (i) mechanical, optical and thermal properties of $B(P,As)_{1-x}N_x$ (x = 0.25, 0.5, 0.75) alloy combinations (ii) hardness behavior of BP and BAs under compression by using Full Potential-Linear Augmented Plane Wave method for the first time.

2. Computational details

The present computations on $B(P,As)_{1-x}N_x$ (x = 0, 0.25, 0.5, 0.75, 1) materials are carried out by means of FP-LAPW method as implemented in the Wien2k code [23] based on density functional theory [24] as in our previous work [25]. In the present study, exchange and correlation effect treated with local density approximation (LDA) [26] and with generalized gradient approximation (GGA) [27] has been applied. The plane wave cut-off of $R_{MT}K_{Max} = 7$ has been chosen, where R_{MT} is the smallest muffin tin sphere radius and k_{max} is being the largest k vector in the plane wave expansion. The R_{MT} of 'B', 'P', 'As' and 'N' are 1.3, 1.61, 1.7 and 1.5 a.u. respectively. Boron Phosphide and Boron Arsenide crystallize in the zinc-blende structure of the space group 216_F-43m. The position of 'B' atom is (0, 0, 0) and 'P', 'As' atom is (0.25, 0.25, 0.25). k-sampling has been done to identify the consistency in total energy and 10 × 10 × 10 k—points has been chosen in the present calculation. The chosen R_{MT} is used to minimize the charge leakage and energy. The self-consistent calculations have been carried out until the difference in the total energy and charge did not exceed 0.0001 mRy and 0.001 e respectively. Volume optimization is done for the compound both BP and BAs where the initial structure file is generated with experimental lattice parameter as reported in the literature [9, 15, 16]. Then, a supercell of size 2 × 2 × 2 is generated for BP (BAs) and in this super cell there will be eight boron and eight phosphorus atoms. When two phosphorus (arsenic) atoms are replaced with two nitrogen atoms, we get $B(P/As)_{.75}N_{.25}$ combination; similarly replacement of four and six phosphorus (arsenic) atoms with the respective number of nitrogen atoms, one will get $B(P/As)_{.5}N_{.5}$ and $B(P/As)_{.25}N_{.75}$ combinations. Volume optimization and fitting in Birch–Murnaghan [28] equation of states gives the optimized lattice parameters for each of $B(P,As)_{1-x}N_x$ alloys (where x = 0.25, 0.5, 0.75). The crystal structures are drawn using xCrysden [29]. Elast package contributed by Thomas Charpin and Mortaza Jamal [30] as implemented in the Wien 2 k code has been applied to each of $B(P,As)_{1-x}N_x$ combination in order to find the respective stiffness coefficients namely C_{11}, C_{12} and C_{44}. The computations are repeated on both BP and BAs in order to generate the structural file under each compression namely at $V/V_0 = 1$, 0.95, 0.9, 0.85, 0.8, 0.7 and 0.6 with the respective optimized lattice constant and the corresponding elastic constants are computed.

3. Results and discussion

3.1. Structural properties of $B(P,As)_{1-x}N_x$ (x = 0, 0.25, 0.5, 0.75, 1) alloys

The obtained optimized structural parameters such as lattice parameters (a_{opt}), space group and density of each of $B(P,As)_{1-x}N_x$ (x = 0, 0.25, 0.5, 0.75, 1) alloy combinations by GGA and LDA schemes are given in Table 1. The analysis of Table 1 shows that there is a good agreement in the optimized lattice parameter values with the existing literature values. As the concentration of nitrogen increases in $B(P,As)_{1-x}N_x$ (x = 0, 0.25, 0.5, 0.75, 1) alloy combinations, (i) it is found that the 'a_{opt}' value decreases and this may be due to the replacement of larger atom namely 'P/As' by 'N'. (ii) Density of $B(P)_{1-x}N_x$ alloy combination increases whereas the density of $B(As)_{1-x}N_x$ alloy combination decreases. For combinations of x = 0, 0.5, 1 the material behaves as Face Centered Cubic (space group 216) and for the remaining combinations such as x = 0.25, 0.75 the system exists as Simple Cubic (space Group 215). The volume optimization curve for each of $B(P,As)_{1-x}N_x$ (x = 0.25, 0.5, 0.75) alloy combination that is drawn between total energy versus V/V_0 is shown in Fig. 1. Electronic, mechanical, thermal and optical properties of these $B(P,As)_{1-x}N_x$ (x = 0.25, 0.5, 0.75) alloy combination are shown in Tables 2, 3, 5 and 6 respectively. Comparison of mechanical properties of $BP_{.25}N_{.75}$ and $BAs_{.25}N_{.75}$ alloys with c-BN and Diamond is shown in Table 4.

3.2. Electronic properties of $B(P,As)_{1-x}N_x$ (x = 0, 0.25, 0.5, 0.75, 1) alloys

The electronic parameters such as energy gap and Fermi energy of $B(P,As)_{1-x}N_x$ (x = 0.25, 0.5, 0.75) alloys are listed in Table 2. From the Table 2, it is observed that the band gap (E_g) at 'Γ' decreases from 1.2 eV (BP) to 0.06 eV ($BP_{.75}N_{.25}$) and then it gradually increases to 1.4 eV ($BP_{.5}N_{.5}$), 2 eV ($BP_{.25}N_{.75}$), 4.5 eV (BN). The same trend is observed in the case of BAs compound. The band structure of $B(P,As)_{.75}N_{.25}$, $B(P,As)_{.5}N_{.5}$ and $B(P,As)_{.25}N_{.75}$ ternary alloys are plotted and are shown in Fig. 2. In $B(P,As)_{.5}N_{.5}$ and $B(P,As)_{.25}N_{.75}$ alloys, the bands are not crossing the Fermi Energy level and therefore it

Table 1 Structural parameters of each of $B(P,As)_{1-x}N_x$; (x = 0, 0.25, 0.5, 0.75, 1) alloy combinations by GGA and LDA schemes

Compound	a (Å)	ρ (g/cm^3) (GGA)	Space group
BP	(Exp) 4.538[a–c]	2.9486[i]	216—Fm3m
	a_{opt} = 4.5489[i], 4.4912[j]	2.962[d]	
	4.551[e,d], 4.558[f], 4.554[h]		
$BP_{.75}N_{.25}$	4.4004[i], 4.342[j]	2.9267[i]	215—Pm3m
	4.400[e]		
$BP_{.5}N_{.5}$	4.2005[i], 4.1449[j]	2.9845[i]	216—Fm3m
	4.210[e]		
$BP_{.25}N_{.75}$	3.9583[i], 3.9082[j]	3.1123[i]	215—Pm3m
	3.960[e]		
BN	(Exp) 3.615[b]	3.4533[i]	216—Fm3m
	3.6275[i], 3.5835[j]	3.475[d]	
	3.626[e], 3.606[f], 3.627[d]		
BAs	a_{exp} = 4.777[a]	5.1248[i]	216—Fm3m
	a_{rep} = 4.8076[i], 4.733[j]	5.139[d]	
	4.83[i(g)], 4.76[j(g)], 4.812[d–e]		
$BAs_{.75}N_{.25}$	4.6239[i], 4.5493[j]	4.7370[i]	215—Pm3m
	4.63[g]		
$BAs_{.5}N_{.5}$	4.3775[i], 4.309[j]	4.3769[i]	216—Fm3m
	4.39[g]		
$BAs_{.25}N_{.75}$	4.0596[i], 4.0021[j]	3.9757[i]	215—Pm3m
	4.07[g]		
BN	(Exp) 3.615[b]	3.4548[i]	216—Fm3m
	3.6270[i], 3.5847[j]		
	3.626[e], 3.606[f], 3.627[d]	3.475[d]	

[a] Ref. [31], [b] Ref. [32], [c] Ref. [33], [d] Ref. [34], [e] Ref. [20], [f] Ref. [5], [g] Ref. [19], [h] Ref. [35]
Present values [i] (GGA), [j] (LDA)

confirms their semiconducting/insulating behaviour; whereas in the case of $B(P,As)_{.75}N_{.25}$, the valence and conduction bands overlap slightly at the Fermi level. Hence it may be stated that there is a possibility of $B(P,As)_{.75}N_{.25}$ alloys to exist as semimetals. Density of states (DOS) histograms and charge density plots are drawn for $B(P,As)_{1-x}N_x$ (x = 0.25, 0.5, 0.75) alloys and are shown in Figs. 3 and 4. From the analysis of DOS histograms, 'N'-2p states contribute towards the total DOS and the covalent nature of $B(P,As)_{.25}N_{.75}$ alloy is revealed in their respective charge density plots (Fig. 4) as there are uniformly distributed directional charge density contours that encloses P–N–B in '$BP_{.25}N_{.75}$' and As–N–B in '$BAs_{.25}N_{.75}$' alloy.

3.3. Mechanical properties of $B(P,As)_{1-x}N_x$ (x = 0, 0.25, 0.5, 0.75, 1) alloys

The linear variation of Voigt elastic coefficients with the concentration of 'N' in the present alloys are obtained both by GGA and LDA scheme and are shown in Fig. 5. Bulk modulus (B), shear modulus (G_H), and Young's modulus (Y) of $B(P,As)_{1-x}N_x$ (x = 0, 0.25, 0.5, 0.75, 1) alloys are depicted in Fig. 6. Zener anisotropy factor (A), Kleinmann Parameter (ξ), Cauchy (C_a) ratio, Born (B_o) ratio and plasticity (B/C_{44}) of $B(P,As)_{1-x}N_x$ (x = 0, 0.25, 0.5, 0.75, 1) alloys are shown in Fig. 7. Poisson's ratio (σ), Pugh's ratio (G/B), Cauchy pressure (C_{12}–C_{44}), Vicker's micro hardness (H_V) of $B(P,As)_{1-x}N_x$ (x = 0, 0.25, 0.5, 0.75, 1) alloys are listed in Table 3 and are verified with existing literature of the parent compounds.

3.3.1. Elastic stiffness coefficients and various moduli

For the present ternary alloy combinations namely $B(P,As)_{1-x}N_x$ (x = 0, 0.25, 0.5, 0.75, 1), the analysis of Voigt elastic coefficients (Fig. 5), shows that they satisfy the stability criteria, namely $C_{11} > 0$, $C_{44} > 0$, $(C_{11} - C_{12}) > 0$, $(C_{11} + 2C_{12}) > 0$ and $C_{12} < B < C_{11}$ [43–45]. From Fig. 5, it is inferred that the curve drawn between concentration of N versus C_{12} is steeper than that is drawn with C_{11} and C_{44}. The Voigt elastic constants obtained by LDA are found to be higher than that of GGA.

From Fig. 6, one can observe that in each of $B(P,As)_{1-x}N_x$ (x = 0, 0.25, 0.5, 0.75, 1) alloy

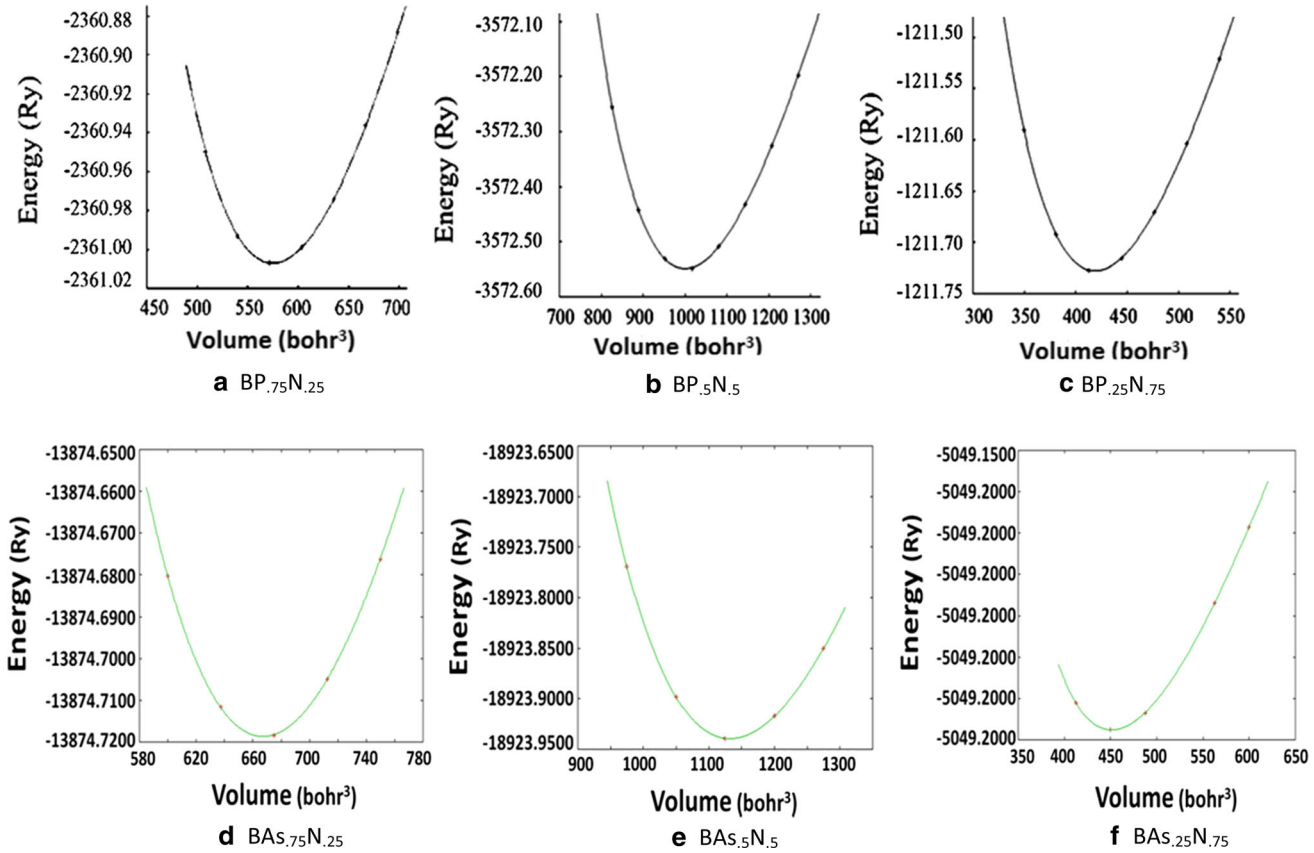

Fig. 1 Volume optimization curve for each of $B(P,As)_{1-x}N_x$; (x = 0.25, 0.5, 0.75) alloy combinations

combination, the profile of each modulus with 'concentration of nitrogen' is observed to be similar. Further one can state that the bulk modulus value increases as one move from BP—$BP_{.75}N_{.25}$—$BP_{.5}N_{.5}$—$BP_{.25}N_{.75}$—BN and also from BAs—$BAs_{.75}N_{.25}$—$BAs_{.5}N_{.5}$—$BAs_{.25}N_{.75}$—BN. The maximum bulk modulus value is obtained for $BP_{.25}N_{.75}$ (267 GPa) combination and its lattice constant is the smallest among the other alloys (Table 1). The Young's modulus and shear modulus values in Fig. 6 reveals that the stiffness and hardness increases as one move from BP—$BP_{.75}N_{.25}$—$BP_{.5}N_{.5}$—$BP_{.25}N_{.75}$—BN alloy and from BAs—$BAs_{.75}N_{.25}$—$BAs_{.5}N_{.5}$—$BAs_{.25}N_{.75}$—BN. Further, it is observed that in each of $B(P,As)_{1-x}N_x$ (x = 0, 0.25, 0.5, 0.75, 1) alloy combination, the shear and bulk modulus values are almost the same value. It is inferred that if B = G, then one will get the Poisson's ratio will be of the order of 0.1 [46] and they exhibit covalent nature. The lower Poisson's values suggest [46] that a large volume change is associated with its deformation.

3.3.2. *Ductile–brittle nature*

The variation in Poisson's ratio, Cauchy pressure and G/B ratio with the concentration of N in both BP and BAs is shown in Table 3. For the present $B(P,As)_{1-x}N_x$ (x = 0, 0.25, 0.5, 0.75, 1) alloys,

(i) Cauchy's pressure values are negative and hence they are of brittle nature. Of all the alloy combinations, $B(P,As)_{.25}N_{.75}$ material is more brittle.
(ii) G/B ratio ranges from 0.93 to 0.98; hence they are of brittle nature.
(iii) σ value ranges from 0.13 to 0.15. Hence the proposed ternary alloys are of brittle nature.

From the above study, one can confirm that all six ternary compounds namely $BP_{.75}N_{.25}$, $BP_{.5}N_{.5}$, $BP_{.25}N_{.75}$ and $BAs_{.75}N_{.25}$, $BAs_{.5}N_{.5}$, $BAs_{.25}N_{.75}$ are of brittle nature, of which $B(P,As)_{.25}N_{.75}$ materials are more brittle than the other.

3.3.3. *Measure of plasticity, Zener anisotropy factor (A), Kleinman parameter (ξ), Cauchy (C_a) and Born (B_o) ratio*

The ratio of the bulk modulus and C_{44} predict the measure of plasticity [47]. Larger values of this ratio indicates the excellent lubricating property offered by that material [44]. For an example, Graphite [48] is found to have 'the

Table 2 Electronic properties of $B(P,As)_{1-x}N_x$; (x = 0, 0.25, 0.5, 0.75, 1) alloy combinations by GGA schemes

Compound	E_g (eV)	E_F (Ry)
BP	Exp. 2.4[a]	0.6116
	1.257[i]	
	1.252[b], 1.25[c]	
$BP_{.75}N_{.25}$	0.06[i]	0.5747
	0.062[b]	
$BP_{.5}N_{.5}$	1.436[i]	0.5949
	0.376[b]	
$BP_{.25}N_{.75}$	2.189[i]	0.6007
	1.934[b]	
BN	Exp. 6.4[e]	0.6872
	4.456[i]	
	4.45[b–c]	
BAs	Exp.0.67[f]	0.5967
	1.212[i]	
	1.206[b], 1.23[c], 1.41[d]	
$BAs_{.75}N_{.25}$	0.03[i]	0.5535
	0.086[b], 0.03[d]	
$BAs_{.5}N_{.5}$	1.288[i]	0.5730
	0.522[b], 0.3[d]	
$BAs_{.25}N_{.75}$	2.279[i]	0.5823
	2.041[b], 1.99[d]	
BN	Exp. 6.4[e]	0.6876
	4.457[i]	
	4.45[b–d]	

[a] Ref. [32], [b] Ref. [20], [c] Ref[17], [d] Ref. [19], [e] Ref. [31], [f] Ref. [36] and [I] (GGA)

measure of plasticity' as 56.1 and it is identified as a good lubricant. Hence, the present ternary alloy system may not serve as good lubricants as the above ratio ranges from 0.83 to 0.89 (Fig. 7).

The Zener anisotropy factor for the cubic crystals is calculated using the formula [49],

$$A = \frac{2C_{44}}{C_{11} - C_{12}} \tag{1}$$

If $A < 1$, the crystal is stiffest along $\langle 100 \rangle$ cube axes and when $A > 1$, it is stiffest along the $\langle 111 \rangle$ body diagonals. If $A = 1$, the crystal is elastically isotropic and is uniformly deformable along all the directions of the body [50]. For the present $B(P,As)_{1-x}N_x$ (x = 0.25, 0.5, 0.75) alloys, the Zener anisotropy factor values range from 1.43 to 1.57 which clearly indicates that these ternary alloys are of anisotropic nature and the degree of stiffness will vary along the $\langle 111 \rangle$ body diagonals.

The bulk modulus values can also be correlated to the anisotropic nature of the given material. If the anisotropy value is closer to unity for a given material then the corresponding bulk modulus value is found be larger. In the present work, the anisotropy values (Fig. 7) of ternary alloys namely $B(P,As)_{1-x}N_x$ (x = 0, 0.25, 0.5, 0.75, 1) decrease towards unity as the nitrogen concentration increases. Here one can witness from the same figure that the bulk modulus value is maximum only for $BP_{.25}N_{.75}$ (A = 1.434).

The condition of minimum energy [50–52] is characterised by the Kleinman parameter and it is calculated by the relation,

$$\xi = \frac{C_{11} + 8C_{12}}{7C_{11} + 2C_{12}} \tag{2}$$

Here $\xi = 0$ indicates no internal displacement and $\xi = 1$ indicates the existence of internal displacement alone [53]. For the present ternary alloy combinations $B(P,As)_{1-x}N_x$ (x = 0.25, 0.5, 0.75), the Kleiman parameter values (Fig. 7) range from 0.39 to 0.41.

The elastic stiffness constants are related by the Cauchy (C_a) and Born (B_o) ratio for the cubic crystals by the following relation [54],

$$C_a = \frac{C_{11}}{C_{44}} \tag{3}$$

$$B_o = \frac{(C_{11} + C_{12})^2}{4C_{11}(C_{11} - C_{44})} \tag{4}$$

From Fig. 7, one can find that the Cauchy ratio increases from $B(P/As)_{.75}N_{0.25}$—$B(P/As)_{.5}N_{.5}$—$B(P/As)_{.25}N_{.75}$ ternary alloys where as Born ratio decreases in the same order.

3.3.4. *Hardness*

Hardness of a given material can be calculated by using various experimental and theoretical available methods [55]. Here, the Vicker's micro hardness is calculated by using Chen's formula [38, 56] given by,

$$H_V = 0.92\ K^{1.137} G^{0.708}, \quad \text{where} \quad K = G/B. \tag{5}$$

The calculated microhardness by both GGA and LDA are presented and compared with available experimental and theoretical microhardness. The variation in microhardness for $B(P,As)_{1-x}N_x$ (x = 0, 0.25, 0.5, 0.75, 1) alloy combination with 'concentration of nitrogen' is shown in Table 3 and it is found that the microhardness value increases with increase in 'concentration of nitrogen'. The microhardness value ranges from 29 to 45 GPa for the ternary alloys under present study and is found to be greater than 40 GPa for $BP_{.25}N_{.75}$ and $BAs_{.25}N_{.75}$ alloys. Hence $BP_{.25}N_{.75}$ and $BAs_{.25}N_{.75}$ alloys could serve as superhard materials. The calculated hardness values are consistent in both

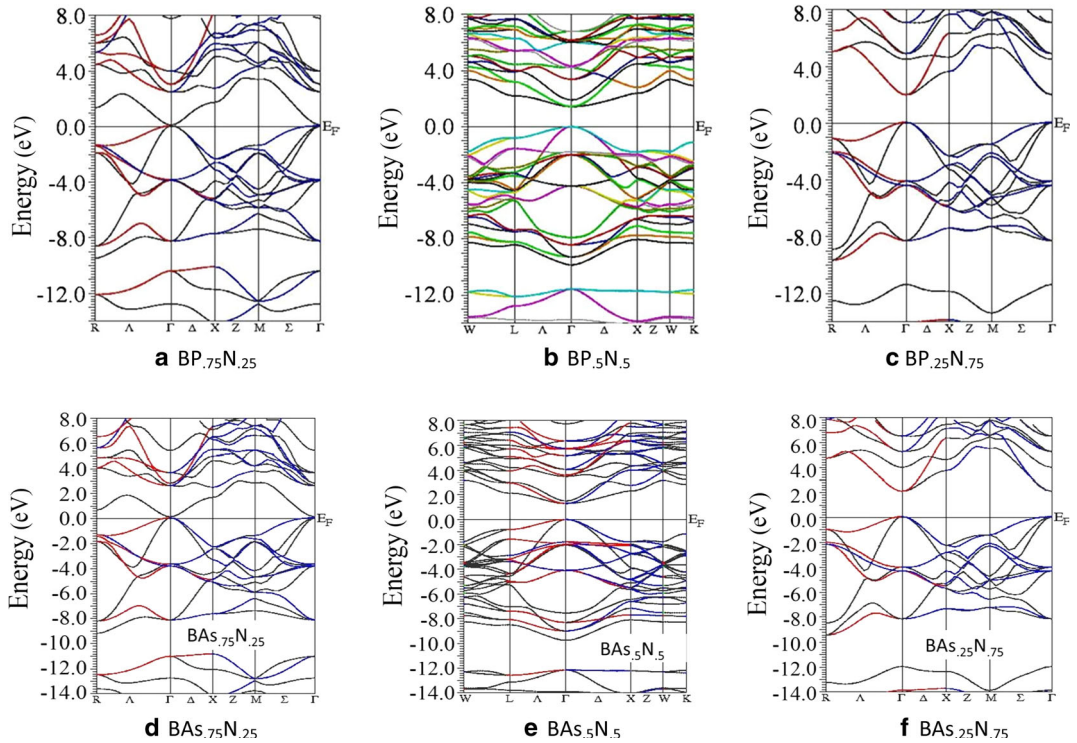

Fig. 2 Band structure of each of $B(P,As)_xN_{1-x}$; (x = 0.25, 0.5, 0.75) alloy combinations

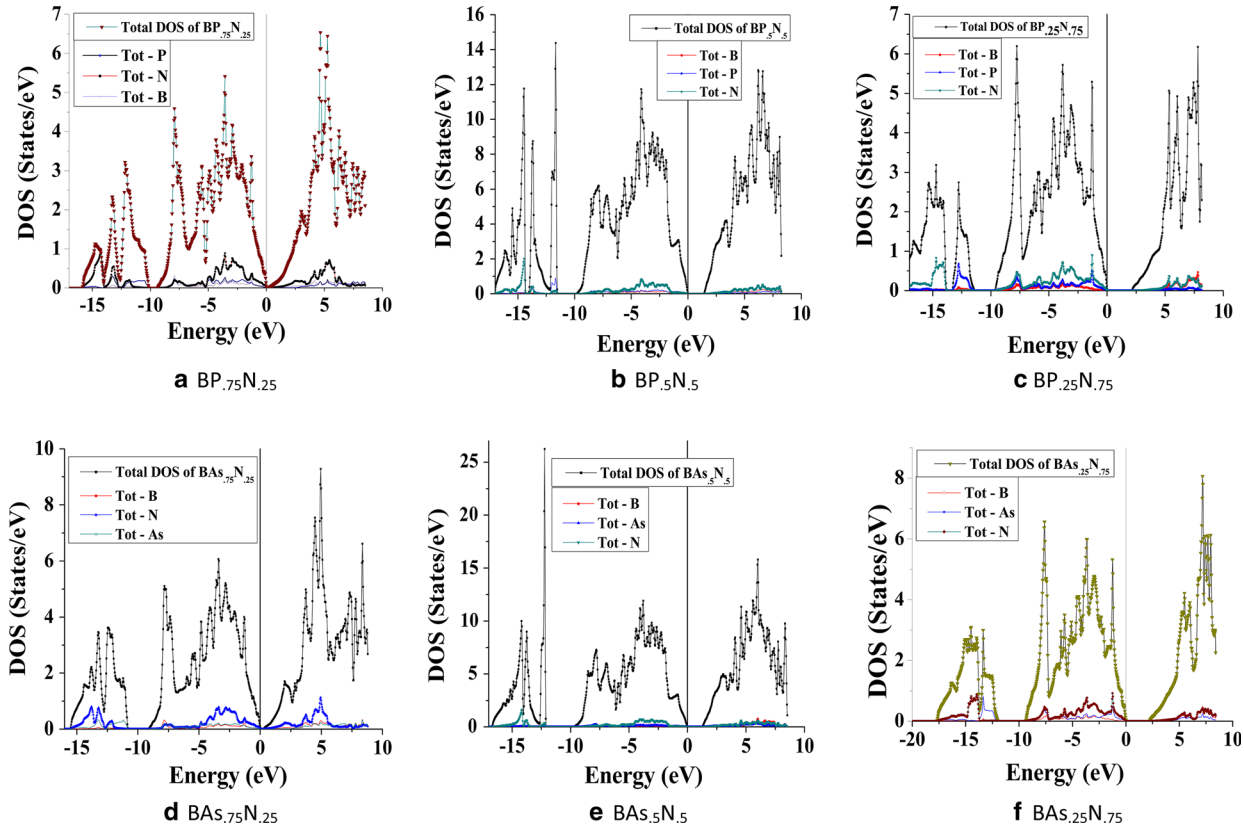

Fig. 3 Density of states histogram for each of $B(P,As)_{1-x}N_x$; (x = 0.25, 0.5, 0.75) alloy combinations

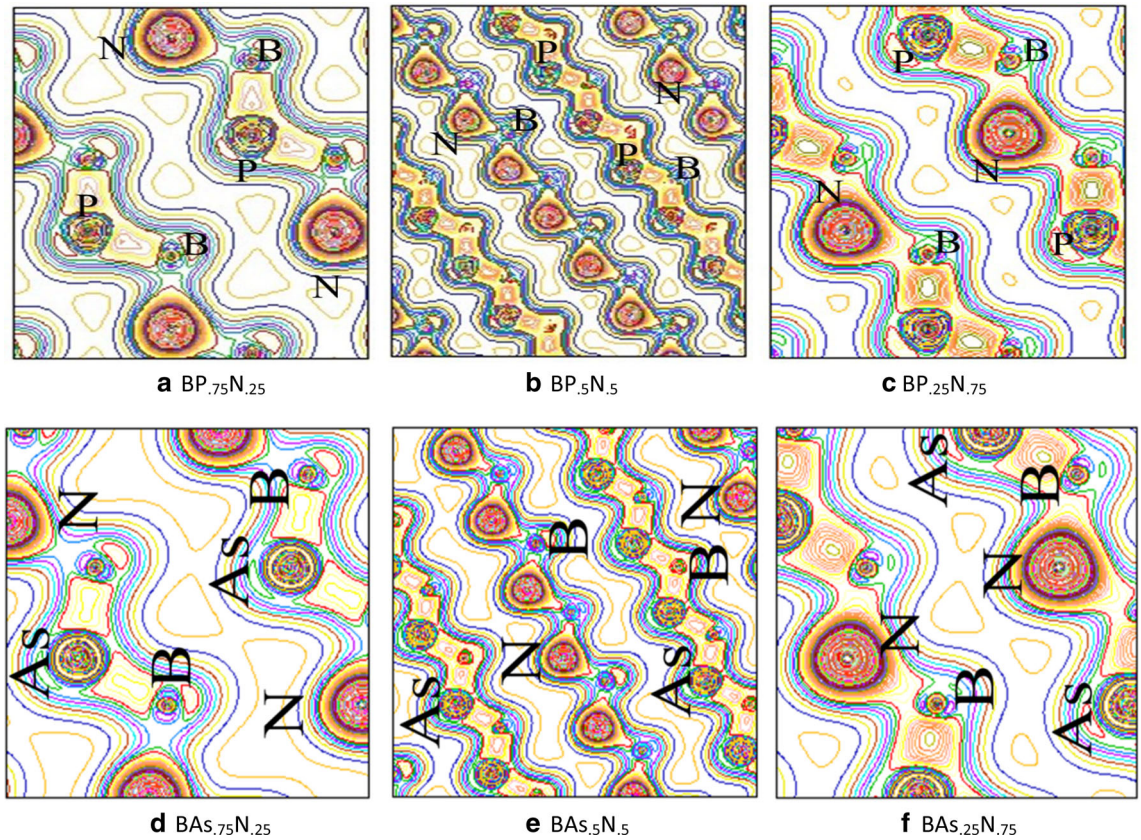

Fig. 4 Charge density plot for each of $B(P,As)_{1-x}N_x$; (x = 0.25, 0.5, 0.75) alloy combinations along (001) plane

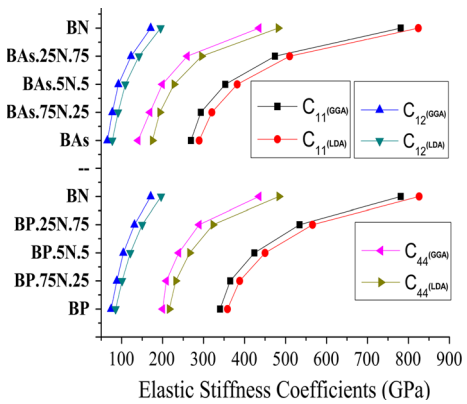

Fig. 5 Elastic stiffness coefficients of each of $B(P,As)_{1-x}N_x$; (x = 0, 0.25, 0.5, 0.75, 1) alloy combinations

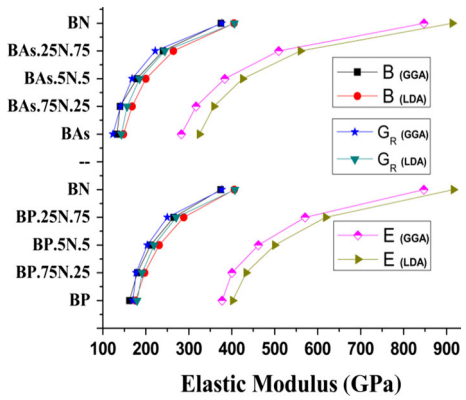

Fig. 6 Elastic modulus of each of $B(P,As)_{1-x}N_x$; (x = 0, 0.25, 0.5, 0.75, 1) alloy combinations

GGA and LDA method. The enhancement of hardness, reduction of lattice constants, enhancement of directional bonding, least value of Poisson's ratio (<0.25) in $B(P,As)_{1-x}N_x$ (x = 0, 0.25, 0.5, 0.75, 1) alloy combinations suggest the possibility of these materials to be [53] indexed as conventional hard materials. In this present work, the maximum hardness is about 43 GPa in the case of $BP_{1-x}N_x$ (x = 0.75) alloy.

3.4. Structural and hardness properties of compounds BP and BAs under compression

Calculations are further extended to study the hardness of BP and BAs at ambient condition and under compressions namely $V/V_0 = 0.95, 0.9, 0.85, 0.8$ & 0.7. The curve that is drawn between the pressure values and the corresponding calculated lattice parameter values of BP and BAs are

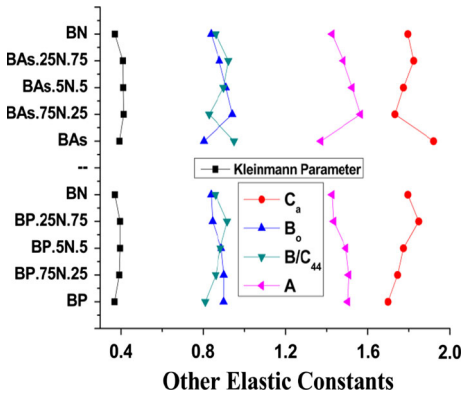

Fig. 7 Other elastic constants such as C_a, B_o, A, B/C_{44} and ξ for each of $B(P,As)_{1-x}N_x$; (x = 0, 0.25, 0.5, 0.75, 1) alloy combinations

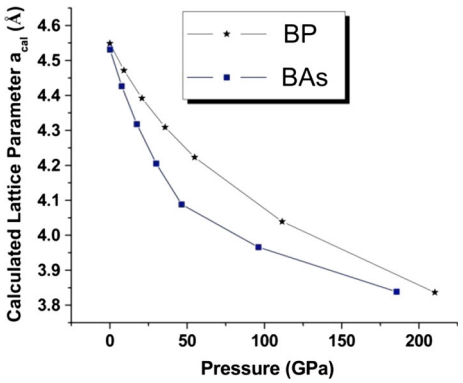

Fig. 8 Pressure versus calculated lattice parameter a_{cal} (Å) of BP and BAs compounds

Table 3 Ductile–Brittle nature and hardness of each of $B(P,As)_{1-x}N_x$; (x = 0, 0.25, 0.5, 0.75, 1) alloy combinations by Jamal elastic package

Compound	σ	C_{12}–C_{44}	G/B	H_v (GPa)	
				GGA	LDA
BP	0.11	−126	1.05	Exp. 33[c]	37
	0.13[a]	−129[b]	1.06[b]	37	
	0.11[b]			31[d]	
$BP_{.75}N_{.25}$	0.13	−121	0.98	35	38
$BP_{.5}N_{.5}$	0.13	−135	0.96	38	39
$BP_{.25}N_{.75}$	0.14	−158	0.94	43	45
BN	0.12	−264	1.01	Exp. 63[c]	65
	0.12[b]	−276[b]	1.02[b]	62	
				64[d]	
BAs	0.14	−75	0.93	Exp. 19[e]	30
	0.12[b]	−98[b]	1.02[b]	26	
				26[d]	
$BAs_{.75}N_{.25}$	0.14	−92	0.95	29	30
$BAs_{.5}N_{.5}$	0.14	−107	0.94	32	34
$BAs_{.25}N_{.75}$	0.15	−137	0.93	39	41
BN	0.12	−264	1.01	Exp. 63[c]	65
	0.12[b]	−276[b]	1.02[b]	62	
				64[d]	

[a] Ref. [37], [b] Ref. [34], [c] Ref. [38], [d] Ref. [39], [e] Ref. [40]

shown in Fig. 8. From Fig. 8, one can state that as the lattice parameter value decreases as the pressure increases.

The study of hardness for BP and BAs is analyzed for the pressure range from ambient condition to 125 GPa and is shown in Fig. 9. The hardness of BP and BAs increases as the pressure increases. The hardness of BP reaches 40 GPa at pressure 20 GPa and reaches a maximum of 47 GPa at 112 GPa. As such getting hardness of more than 40 GPa under very high pressure is of no practical use. But it gives an important clue to the experimentalists for

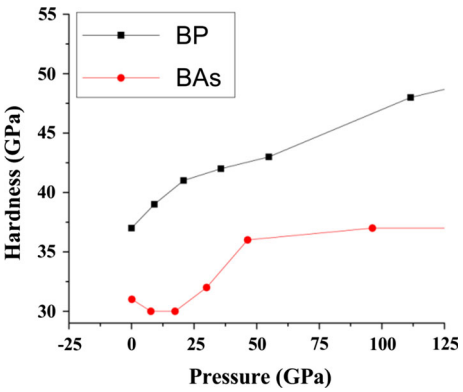

Fig. 9 Hardness versus pressure of BP and BAs under compression

synthesizing the hard phase of BP/BAs. The same pressure effect can be realized by doping with a suitable element in such a way that one could synthesize a material of reduced lattice parameter that matches with that of high pressure; mimicking high pressure is possible.

3.5. Thermal properties of $B(P,As)_{1-x}N_x$ (x = 0, 0.25, 0.5, 0.75, 1) alloys

The lattice vibrations are responsible for the characteristic properties of matter such as specific heat, thermal conductivity, electrical conductivity, optical and dielectric properties, diffusion mechanism, phase change phenomena etc. [57]. Anisotropic materials are directional dependent on all properties including thermal properties. Longitudinal (v_l) and transverse (v_t) wave velocities are the two types of sound elastic waves exist in the solids. We can calculate the average elastic wave velocity (v_m) from v_l and v_t, if we know the crystal density (ρ) and the elastic stiffness coefficients (C_{ij}) [58]. They are calculated using the following relations,

Table 4 Comparison of $B(P,As)_{1-x}N_x$; (x = 0, 0.25, 0.5, 0.75, 1) alloy combinations

Properties/compounds	$BP_{.25}N_{.75}$	$BAs_{.25}N_{.75}$	Diamond	c-BN
a (Å)	3.9583	4.0596	3.56 [41]	3.615 [42]
P (g/cm^3)	3.11	3.98	3.52	3.55
Bonding	Covalent	Covalent	Covalent	Covalent
Ductile/brittle	Brittle	Brittle	Brittle	Brittle
C_{12}–C_{44}	−158	−137	−454	−300
σ	0.14	0.15	0.1	0.11
G/B	0.94	0.93	1.21	1.03
H_V (GPa)	44	40	90	63

Table 5 Thermal properties such as elastic wave velocity, Debye's temperature (θ_D) and melting point (T_m) for each of $B(P,As)_{1-x}N_x$; (x = 0, 0.25, 0.5, 0.75 and 1) alloy combinations

Compound	ν_l (m/s)	ν_t (m/s)	ν_m (m/s)	θ_D (K)	$T_m \pm 300$ (K)
BP	11,479	7591	8302	Exp. 980[c]	Exp. 2800[c]
	11,554[a]	7550[a]	8275[a]	1087	
		7611[b]	8327[b]	1095[a]	2560
	11,490[b]			1090[b]	2560[b]
$BP_{.75}N_{.25}$	11,928	7781	8529	1154	2709
$BP_{.5}N_{.5}$	12,703	8254	9052	1283	3058
$BP_{.25}N_{.75}$	13,867	8965	9838	1480	3707
BN	15,939	10,453	11,451	1880	5167
	16,141[d]	8235[d]	9227[d]	1886[b]	5176[b]
	15,935[b]	10,493[b]	11,489[b]		
BAs	7919	4910	5391	668	2143
	7800[b]	5115[b]	5601[b]	Exp. 625[c]	Exp. 2300[c]
	7373[e]	5039[e]	5490[e]	693[b], 698[e]	2133[b]
					2333[e]
$BAs_{.75}N_{.25}$	8439	5463	5994	772	2286
$BAs_{.5}N_{.5}$	9595	6195	6799	925	2636
$BAs_{.25}N_{.75}$	11,606	7473	8204	1203	3352
BN	15,940	10,452	11,450	1880	5168
	16,141[d]	8235[d]	9227[d]	1886[b]	5176[b]
	15,935[b]	10,493[b]	11,489[b]		

[a] Ref. [11], [b] Ref. [5], [c] Ref. [15], [d] Ref. [16], [e] Ref. [19]

$$\nu_l = \left(\frac{3B + 4G}{3\rho}\right)^{1/2} \tag{6}$$

$$\nu_t = \left(\frac{G}{\rho}\right)^{1/2} \tag{7}$$

$$\nu_m = \left[\frac{1}{3}\left(\frac{2}{\upsilon_t^3} + \frac{1}{\upsilon_l^3}\right)\right]^{-1/3} \tag{8}$$

The calculated Longitudinal (ν_l), transverse (ν_t), average elastic wave velocity (ν_m) and Debye temperature (θ_D) of the present work are tabulated in Table 5. There seems excellent accordance with the available literature. In both the cases of BP and BAs, addition of nitrogen increases the longitudinal and transverse velocities and maximum can be seen for $BP_{.25}N_{.75}$ and $BAs_{.25}N_{.75}$ ternary alloys.

Many of the physical properties of the solid such as specific heat, elastic stiffness constants (C_{ij}), bond strength, melting temperature (T_M), thermal expansion and thermal conductivity are closely related to the Debye temperature (θ_D) of the given material [59]. It is the temperature above which the crystal behaves classically, because the thermal vibrations become more important than the quantum effects. At low temperature, the lattice vibrational excitations arise solely from acoustic modes, i.e., when θ_D is associated with lattice vibrations.

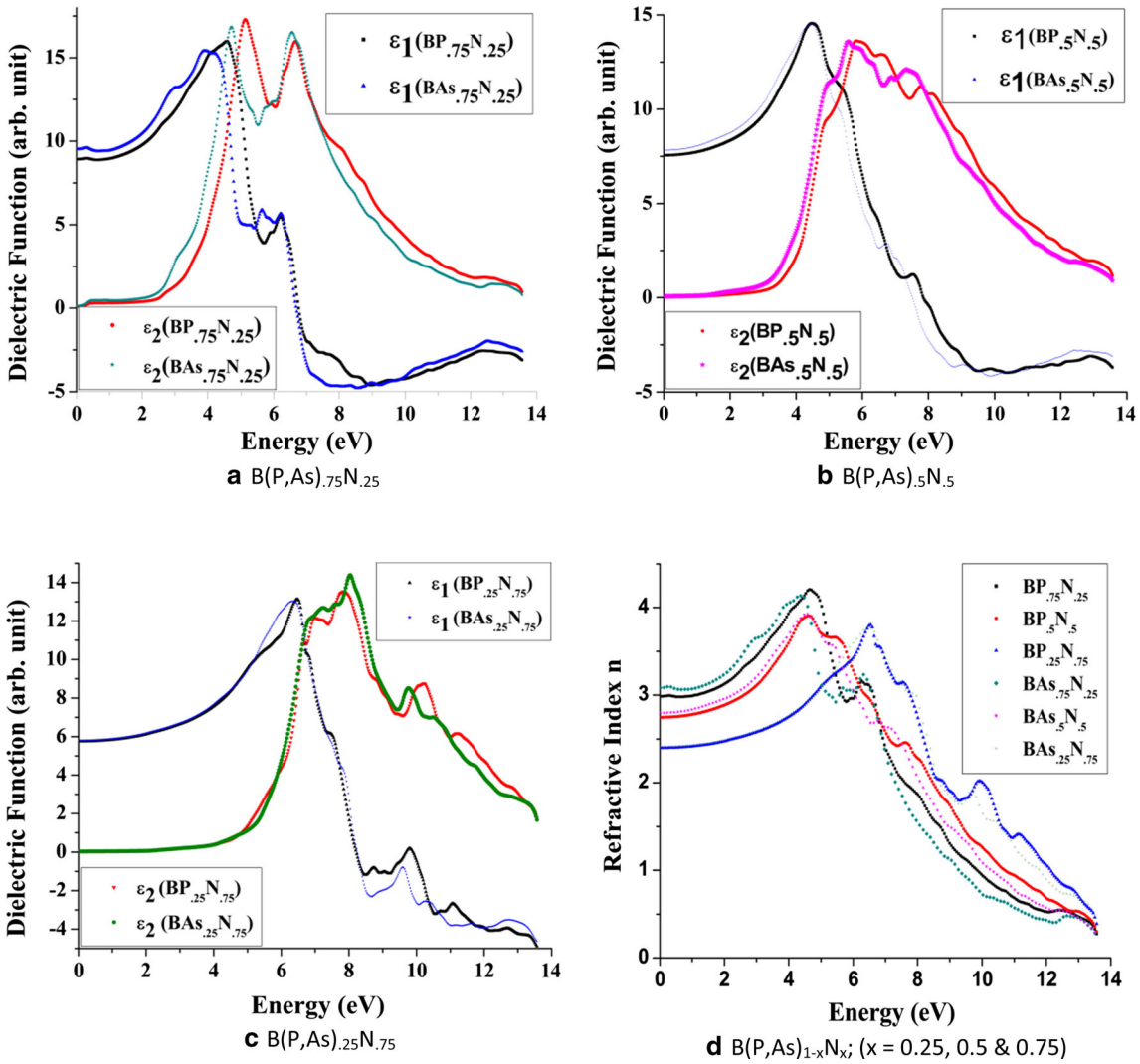

Fig. 10 Real and imaginary part of dielectric function and refractive index of each of $B(P,As)_{1-x}N_x$; (x = 0, 0.25, 0.5, 0.75, 1) alloy combinations

The Debye temperature is obtained through well-established empirical or semi-empirical formulas. One of the semi-empirical formulas [59] can be used to estimate the values of Debye temperature through the averaged elastic wave velocity v_m

$$\theta_D = \frac{h}{k_B}\left(\frac{3}{4\pi V_a}\right)^{1/3} v_m \quad (9)$$

where h is Planck's constant, k_B is Boltzmann's constant, V_a is atomic volume and v_m is average sound wave velocity.

From the Table 5 one can notice that the θ_D values increase as the nitrogen concentration increases in the case of both BP and BAs compound. θ_D value reaches maximum for $BP_{.25}N_{.75}$ (1283 K)and $BAs_{.25}N_{.75}$ (1203 K) ternary alloys. This shows that the thermal conductivities of these alloys are more than that of other ternary alloys in the present work.

Also the melting temperature increases as the θ_D value increases and is maximum of 1480 ± 300 K for $BP_{.25}N_{.75}$ alloys.

3.6. Optical properties of $B(P,As)_{1-x}N_x$ (x = 0, 0.25, 0.5, 0.75, 1) alloys

The optical properties are key tool to study energy band structure of solid which is directly related to complex dielectric function and ε(ω) is determined mainly by the transition between the valence and conduction bands. The imaginary part is obtained directly from the electronic structure calculations. From the result, the real part is determined using the Kramers–Kronig dispersion relation. According to the perturbation theory and Kramers–Kronig relation [17], the real and imaginary part of dielectric function i.e. $\varepsilon_1(\omega)$ and $\varepsilon_2(\omega)$ are expressed as,

Table 6 Optical properties such as real and imaginary dielectric constants, refractive index (n), extinction coefficient (k) and reflectivity (R) for each of $B(P,As)_{1-x}N_x$; (x = 0, 0.25, 0.5, 0.75, 1) alloy combinations

Compound	ε_1	ε_2	n	k	R
BP	9	0	3	0	0.25
	11[a], 10.55[b]	0[a–c]	3[c], 3.25[c–d]		0.28[b]
	9.03[c]				
$BP_{.75}N_{.25}$	8.8	0.1	2.97	0.02	0.246
$BP_{.5}N_{.5}$	7.5	0	2.7386	0	0.216
$BP_{.25}N_{.75}$	5.8	0	2.3987	0	0.169
BN	3.5	0	1.8708	0	0.09
	3.46[f]	0[e–f]	2.17[e], 1.86[f]		
	4.5[e]				
BAs	9.3	0	3.0496	0	0.256
	11.19[b]	0[f,i]	3.35[b,d,g]		
	9.5[h], 9.67[c]		3.07[f], 3.1[c]		
	11.27[i], 9.38[f]				
$BAs_{.75}N_{.25}$	9.0	0.1	3	0.03	0.25
$BAs_{.5}N_{.5}$	7.8	0	2.7929	0.02	0.223
$BAs_{.25}N_{.75}$	5.8	0.2	2.4083	0	0.171
BN	3.5	0	1.8708	0	0.09
	3.46[f], 4.5[e]	0[e–f]	2.17[e], 1.86[f]		

[a] Ref. [1], [b] Ref. [20], [c] Ref. [18], [d] Ref. [2], [e] Ref. [17], [f] Ref. [8], [g] Ref. [6], [h] Ref. [23], [i] Ref. [24]

$$\varepsilon_2(\omega) = \frac{e^2 h}{\pi m^2 \omega^2} \sum_{\upsilon,c} \int_{BZ} |M_{c\upsilon}(k)|^2 \delta[\omega_{cv}(k) - \omega] d^3k, \quad (10)$$

$$\varepsilon_1(\omega) = 1 + \frac{2}{\pi} P \int_0^{\infty} \frac{\omega' \varepsilon_2(\omega')}{\omega'^2 - \omega^2} d\omega', \quad (11)$$

where m, e are the mass and electrical charge of the electron, respectively. The integral is taken over the first Brillouin zone. The momentum dipole elements: $M_{cv}(k) = \langle u_{ck}|\delta\nabla|u_{vk}\rangle$, where δ is the potential vector defining the electric field, are matrix elements for direct transitions between valence—$u_{vk}(r)$ and conduction-band $u_{ck}(r)$ states, and the energy $\hbar\omega_{cv}(k) = E_{ck} - E_{vk}$ is the corresponding transition energy. P implies the principal value of the integral.

The optical dispersion and absorption spectra i.e. real and imaginary parts of the complex dielectric function versus the photon energy for the present $B(P,As)_{1-x}N_x$ (x = 0.25, 0.5 and 0.75) alloys are presented in Fig. 10(a)–10(c). The complex dielectric function can be written as $\varepsilon(\omega) = \varepsilon_1(\omega) + i\varepsilon_2(\omega)$ and is one of the best tool for analyzing band structure and energy gap of the crystalline materials. The static dielectric constant i.e. real part of dielectric function in the zero frequency limit $\varepsilon_1(0)$ is the most important quantity and the values for present alloys are given in Table 6. The results are verified with the literature available and there is a good accordance with the previous results. The value of $\varepsilon_1(0)$ decreases in $BP_{1-x}N_x$ (x = 0.25, 0.5 and 0.75) alloys from 8.8($BP_{.75}N_{.25}$)–7.5($BP_{.5}N_{.5}$)–5.8($BP_{.25}N_{.75}$) and in $BAs_{1-x}N_x$ (x = 0.25, 0.5 and 0.75) alloys from 9.0($BAs_{.75}N_{.25}$)–7.8($BAs_{.5}N_{.5}$)–5.8($BAs_{.25}N_{.75}$). It is clearly implies that $\varepsilon_1(0)$ decreases by increasing the concentration of nitrogen with BP and BAs. The main peaks in the real part of the dielectric spectrum has appeared in low frequency side for the present alloy system at 4.41 eV ($BP_{.75}N_{.25}$), 4.50 eV ($BP_{.5}N_{.5}$), 6.44 eV ($BP_{.25}N_{.75}$), 3.89 eV ($BAs_{.75}N_{.25}$), 4.42 eV ($BAs_{.5}N_{.5}$) and 6.33 eV ($BAs_{.25}N_{.75}$) respectively.

$\varepsilon_2(\omega)$ is some way responsible for optical absorption in materials due to various inter-band transitions and for the present ternary alloys the values are almost zero which shows negligible absorption in the zero frequency limit. The analysis of $\varepsilon_2(\omega)$ spectrum in our present work show that the first critical point i.e. absorption threshold occur at 2.39 eV ($BP_{.75}N_{.25}$), 3.12 eV ($BP_{.5}N_{.5}$), 4.49 eV ($BP_{.25}N_{.75}$), 2.41 eV ($BAs_{.75}N_{.25}$), 3.26 eV ($BAs_{.5}N_{.5}$) and 4.41 eV ($BAs_{.25}N_{.75}$). Optical transitions between top of the valence band maximum and bottom of the conduction band at the Γ point (Γ_V–Γ_C) are responsible for these critical points. The addition of nitrogen increases the direct band gap and hence increases the first critical point energies towards higher energies. Other than critical points there are some main peaks exist in the absorption spectra. For the present alloy system, there are three peaks appear at 0.33 eV, 5.15 eV & 6.69 eV for $BP_{.75}N_{.25}$ alloy. As $BP_{.75}N_{.25}$ alloy is semimetal and its band gap is so small, the first peak at 0.33 eV occurs due to direct band transitions at Γ_V–Γ_C. In the case $BP_{.5}N_{.5}$ alloy the main peaks are found at 5.84, 6.56 and 7.75 eV and for $BP_{.25}N_{.75}$ alloy found at 6.99, 7.8 and 10.24 eV. In the case of BAs, the main peaks are appear at 0.41, 4.71 and 6.55 eV for $BAs_{.75}N_{.25}$ alloy, six peaks at 4.97, 5.5, 5.89, 6.30, 6.82 and 7.31 eV for $BAs_{.5}N_{.5}$ alloy and five peaks at 7.2, 7.53, 8.03, 9.7 and 10.49 eV for $BAs_{.25}N_{.75}$ alloy. These peaks occur because of inter-band transitions of top of the valance band to conduction band at different k point.

The other important optical constants known as refractive index (n), reflectivity (R) and the local maxima of the extinction coefficient (k) are obtained using both real and imaginary parts of the dielectric function by the following formulae [11, 60–62],

$$n = \left[\frac{\sqrt{\varepsilon_1^2 + \varepsilon_2^2} + \varepsilon_1}{2}\right]^{1/2} \quad (12)$$

$$k = \left[\frac{\sqrt{\varepsilon_1^2 + \varepsilon_2^2} - \varepsilon_1}{2}\right]^{1/2} \quad (13)$$

$$R = \frac{(n-1)^2 + k^2}{(n+1)^2 + k^2} \quad (14)$$

Semiconductors especially III–V semiconductors are well known for their optoelectronic applications. When light passes through the different substances its velocity decreases by increasing of the refractive index of these substances [63, 64]. The refractive index and band gap are the two fundamental properties that decide the optical and electronic properties of semiconductors. From the Table 6, it is observed that the energy band gap and refractive index of $B(P,As)_{1-x}N_x$ (x = 0, 0.25, 0.5, 0.75, 1) alloys are inversely proportional to each other. One can also found from the same Table that all $\varepsilon_1(0)$, n & R values decrease as the concentration of nitrogen increases in BP and BAs.

4. Conclusion

Structural, electronic, mechanical, thermal and optical properties of $B(P,As)_{1-x}N_x$ (x = 0, 0.25, 0.5, 0.75, 1) compounds at ambient condition using the first principle calculations by both GGA and LDA schemes are studied. Charge density plots show all $B(P,As)_{1-x}N_x$ (x = 0, 0.25, 0.5, 0.75, 1) alloy combinations have highly directional bonding. Band structure and DOS show that $B(P,As)_{1-x}N_x$ (x = 0.5 and 0.75) alloys are semiconductors and they have direct band gap while $B(P,As)_{1-x}N_x$ (x = 0.25) alloys are observed to be semimetals. The bulk, shear and Young's modulus is found to be comparatively more for $BP_{.25}N_{.75}$ (/$BAs_{.25}N_{.75}$)alloy than that of respective $B(P)_{1-x}N_x$ (x = 0.25 and 0.5) (/$B(As)_{1-x}N_x$ (x = 0.25, 0.5 and 0.75) alloys). Hardness of $BP_{.25}N_{.75}$ alloy and $BAs_{.25}N_{.75}$ alloy is computed to be 44 and 40 GPa respectively which makes these alloys to be superhard materials. Since all $B(P,As)_{1-x}N_x$ (x = 0, 0.25, 0.5, 0.75, 1) alloy combinations have highly directional bonding, they exhibit brittle nature. The study of hardness for BP and BAs under compression gives an important clue and impetus to the experimentalists about the possibility of deriving materials of hardness value more than 40 GPa and it could be obtained by doping with a suitable element in such a way that one could synthesize material of reduced lattice parameter that matches with that of high pressure. In both the cases i.e. BP and BAs, addition of nitrogen increases the longitudinal and transverse velocities and maximum can be seen for $BP_{.25}N_{.75}$ and $BAs_{.25}N_{.75}$ ternary alloys. θ_D values increases as the nitrogen concentration increases and reaches maximum for $BP_{.25}N_{.75}$ (1283 K) and $BAs_{.25}N_{.75}$ (1203 K) ternary alloys. The effect of nitrogen addition decreases the refractive index values in both BP and BAs cases.

Acknowledgements The authors are grateful to the DST-SERB Board, India for funding this project through the project reference number SR/S2/CMP-0039/2012 dated 13-02-13.

References

[1] X Jiang, J Zhao and X Jiang, *Computat. Mater. Sci.* **50** 2287 (2011)
[2] S Veprek, *J. Vac. Sci. Technol. A* **17** 2401 (1999)
[3] I Hamdi, N Meskini, *Phys. B* **405** 2785 (2010)
[4] R M Wentzcovitch, K J Chang, M L Cohen, *Phys. Rev. B* **34** 1071 (1986)
[5] R M Wentzcovitch, M L Cohen, P K Lam, *Phys. Rev. B* **36** 6058 (1987)
[6] V A Mukhanov, O O Kurakevych and V L Solozhenko, *J. Superhard Mater.* **30** 6 36 (2008)
[7] Hebbache M, *EPL* **87** 16001 (2009)
[8] Y Kumashiro, T Mitsuhashi, S Okaya, F Muta, T Koshiro, Y Takahashi, M Mirabayashi, *J. Appl. Phys.* **65**(5) 2147 (1989)
[9] V L Solozhenko and V A Mukhanov, *J. Superhard Mater.* **37**(6) 438 (2015)
[10] S Daoud, N Bioud, N Lebgaa, L Belagraa and R Mezouar, *Indian J. Phys.* **87** 355 (2013)
[11] A Zaoui, S Kacimi, A Yakoubi, B Abbar, B Bouhafs, *Phys. B* **367** 195 (2005)
[12] V A Mukhanov, P S Sokolov, Y Le Godec, V L Solozhenko, *J. Superhard Mater.* **35**(6) 415 (2013)
[13] S Daoud, K Loucif, N Bioud, N Lebgaa, L Belagraa, *Pramana* **79**(1) 95 (2012)
[14] E-S Oh, *Met. Mater. Int.* **17**(1) 21 (2011)
[15] A Riane, A Zaoui, M Certier, H Aourag, *Physica B* **252** 229 (1998)
[16] M Merabet, D Rached, R Khenata, S Benalia, B Abidri, N Bettahar, S Bin Omran, *Phys. B* **406** 3247 (2011)
[17] A Zaoui and F El Haj Hassan, *J. Phys. Condens. Matter* **13** 253 (2001)
[18] S Bagci, S S Duman, H M Tütüncü and G P Srivastava *PRB* **79** 125326 (2009)
[19] M Guemou, A Abdiche, R Riane, R Khenata, *Phys. B* **436** 33 (2014)
[20] F El Haj Hassan, H Akbarzadeh, *Mater. Sci. Eng. B* 121 170 (2005)
[21] A Bouhemadou, R Khenata, M Kharoubi, T Seddik, Ali H Reshak and Y Al-Douri, *Comput. Mater. Sci.* **45** 474 (2009)
[22] A Abdiche, R Riane, M Guemou, R Khenata, R Moussa, G Murtaza and S Bin Omran, *Solid State Commun* **206** 56 (2015)
[23] P Blaha, K Schwarz,G Madsen, D Kvasnicka and J Luitz, 2001 Wien2k—An Augmented Plane Wave + Lo Program for Calculating Crystal Properties. ISBN-3-95010131-1-1
[24] W Kohn, L J Sham *Phys. Rev.* **140** A1133 (1965)
[25] M Sundareswari, D S Jayalakshmi, E Viswanathan *Philos Mag* **96**(5) 511 (2016)
[26] J P Perdew, Y Wang *Phys. Rev. B* **45**(13) 244 (1992)
[27] P Perdew, S Burke, M Ernzerhof, *Phys. Rev. Lett.* **77** 3865 (1996)
[28] F D Murnaghan, *Proc. Natl. Acad. Sci. USA* **30** 244 (1947)
[29] A Kokalj, *Comput. Mater. Sci.* **28** 155 (2003)
[30] Jamal M, 2012 Cubic-Elastic, http://www.wien2kat/reg_user/unsupported/cubic-elast/(2012)

[31] Landolt H, Börnstein R, Hellwege K H, Manfred Böhn, Schulz M, Harald Weiss and Madelung O, *Landolt-Bornstein New Series*, Group III, Vol 17, Part A (Springer, Berlin) (1982)
[32] E Knittle, R M Wentzcovitch, R Jeanloz and M L Cohen *Nature* **337** 349 (1989)
[33] W Wettling and J Windscheif, *Solid State Commun.* **50** 33 (1984)
[34] M Ustundag, M Aslan, Battal G M Yalcin, *Comput. Mater. Sci* **81** 471 (2014)
[35] H Meradji, S Drablia, S Ghemid, H Belkhir, B Bouhafs and A Tadjer, *Phys. Stat. Sol.* B **241**, 2881 (2004)
[36] H Bross, R Bader, *Phys. Stat. Sol. B* **191** 369 (1995)
[37] R Hill, *Proc. Phys. Soc. A* 65 349 (1952)
[38] FM Gao, JL He, ED Wu, SM Liu, DL Yu, DC Li, *Phys. Rev. Lett.* **91** 015502 (2003)
[39] Y Tian, B Xu, Z Zhao *Int. J. Refract. Metals Hard Mater.* **33** 93 (2012)
[40] A Simunek, J Vackar, *Phys. Rev. Lett.* **96** 085501 (2006)
[41] E Güler and M Güler *Chin. J. Phys.* **53** 2 (2015)
[42] M Fatmi, B Ghebouli, M A Ghebouli and Z K Hieba, *Phys. Scr.* **83** 065702 (2011)
[43] M Sundareswari, S Ramasubramanian, M Rajagopalan, *Solid State Commun.* **150** 2057 (2010)
[44] M Born and K Huang, *Dynamical Theory of Crystal Lattices* (Oxford: Clarendon Press) (1956)
[45] E Güler, M Güler, *Int. J. Multiphys.* **7**(2) 95 (2013)
[46] Y L Hao, S J Li, B B Sun, M L Sui and R Yang, *PRL* **98** 216405 (2007)
[47] L Vitos, P A Korzhavyi, B Johansson *Nat. Mater.* **2** 25 (2003)
[48] Z Sun, D Music, R Ahuja and J M Schneider *PRB* **71** 193402 (2005)
[49] S Daoud, K Loucif, N Bioud, N Lebgaa *J. Acta Phys. Pol. A* **122**(1) 109 (2012)
[50] M Balkanski and R F Wallis, *Semiconductor Physics and Applications* (Oxford: Oxford UniversityPress), pp 149–150 (2000)
[51] D Powell, M A Migliorato and A G Cullis. *PRB* **75** 115202 (2002)
[52] H Zhao, A Chang and Y Wang *J. Phys.* **404** 2192 (2009)
[53] Newnham R E, *Properties of Materials, Anisotropy, Symmetry, Structure* (Oxford: Oxford University Press), pp 45–87 (2005)
[54] S Adachi *Physical Properties of III–V Semiconductor Compounds* (New York: Wiley), pp 20–26 (1992)
[55] A R Oganov, A O Lyakhov *J. Superhard Mater.* **32**(3) 143 (2010)
[56] Chen X-Q, Niu H, Li D, Li Y, *Intermetallics*, **19** 1275 (2011)
[57] Y-L Chen, D-P Yang *Mössbauer Effect in Lattice Dynamics: Experimental Techniques and Applications.* (Weinheim: Wiley-VCH) (2007)
[58] W Huang and H Chen *Phys. B* 449 133 (2014)
[59] D K Kerry, *Semiconductors* (New York: Macmillan Publishing Company) (1991)
[60] A Denin, A O Eriksson, R Ahuja, B Johansson, M S Brooks, T Gasche et al, *Phys. Rev. B* **54** 1673 (1996)
[61] M Fox, *Optical Properties of Solids* (New York: Oxford University Press) (2001)
[62] M Dressel and G Gruner, *Electrodynamics of Solids: Optical Properties of Electrons in Matter* (Cambridge: Cambridge University Press) 2002
[63] N M Ravindra, P Ganapathy and J Choi, *Infrared Phys. Technol.* **50** 21 (2007)
[64] L Hamioud, A Boumaza, S Touam, H Meradji, S Ghemid, F El Haj Hassan, R Khenata and S Bin Omran, *Philos. Mag.* **96**(16) 1694 (2016)